

9-Substituted 6,6-Dimethyl-11-oxo-6,11-dihydro-5H-benzo[*b*]carbazoles as Highly Selective and Potent Anaplastic Lymphoma Kinase Inhibitors

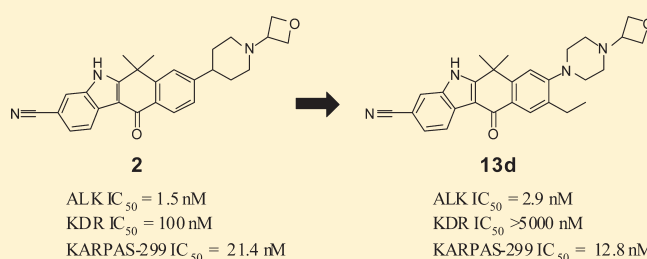
Kazutomo Kinoshita,^{*,†} Takamitsu Kobayashi,[†] Kohsuke Asoh,[†] Noriyuki Furuichi,[†] Toshiya Ito,[†] Hatsuo Kawada,[†] Sousuke Hara,[†] Jun Ohwada,[†] Kazuo Hattori,[†] Takuho Miyagi,[†] Woo-Sang Hong,[‡] Min-Jeong Park,[‡] Kenji Takanashi,[†] Toshiyuki Tsukaguchi,[†] Hiroshi Sakamoto,[†] Takuo Tsukuda,[†] and Nobuhiro Oikawa[†]

[†]Research Division, Chugai Pharmaceutical Co., Ltd., 200 Kajiwara, Kamakura, Kanagawa 247-8530, Japan

[‡]C&C Research Laboratories, 146-141, Annyeong-dong, Hwaseong-si, Gyeonggi-do 445-380, Republic of Korea

Supporting Information

ABSTRACT: 9-Substituted 6,6-dimethyl-11-oxo-6,11-dihydro-5H-benzo[*b*]carbazoles were discovered as highly selective and potent anaplastic lymphoma kinase (ALK) inhibitors by structure-based drug design. The high target selectivity was achieved by introducing a substituent close to the E₀ region of the ATP binding site, which has a unique amino acid sequence. Among the identified inhibitors, compound **13d** showed highly selective and potent inhibitory activity against ALK with an IC₅₀ value of 2.9 nM and strong antiproliferative activity against KARPAS-299 with an IC₅₀ value of 12.8 nM. The compound also displayed significant antitumor efficacy in an established ALK fusion gene-positive anaplastic large-cell lymphoma (ALCL) xenograft model in mice without body weight loss.



INTRODUCTION

Anaplastic lymphoma kinase (ALK) is a receptor tyrosine kinase (RTK) belonging to the insulin receptor superfamily, which includes insulin-like growth factor-1 receptor (IGF-1R) and leukocyte tyrosine kinase (LTK). The function of ALK in the normal human body is unclear. A possible role of ALK is in physiological development, and its expression in normal tissues is very restricted to the central nervous system.^{1,2} The kinase was originally identified as a part of the fusion oncogene nucleophosmin (NPM)-ALK resulting from a t(2;5) chromosomal translocation in anaplastic large cell lymphomas (ALCL).³ NPM-ALK is detected in approximately 75% of all ALK-positive ALCL and is implicated in the pathogenesis of ALCL.⁴ Not only NPM-ALK but also other ALK fusion genes have been identified in ALCL,⁵ inflammatory myofibroblastic tumor (IMT),⁶ diffuse large B-cell lymphoma (DLBCL),⁷ squamous cell carcinoma (SCC),⁸ and nonsmall cell lung cancer (NSCLC).⁹ It is noteworthy that echinoderm microtubule-associated protein-like 4 (EML4)-ALK in NSCLC was the first fusion gene found to be an oncogenic factor in solid tumors.¹⁰ EML4-ALK has been detected in approximately 5% of NSCLC patients¹¹ and is mutually exclusive for known oncogenic mutated-EGFR and KRAS.¹² In addition, genetic amplification and overexpression of ALK have recently been discovered to cause childhood neuroblastoma.^{13,14} These findings indicate that ALK is an attractive drug target for treatment of various ALK-positive cancers in blood and solid tumors.

The inhibition of particular kinases is considered to have risk of adverse events. For example, inhibitions of KIT and KDR have been elucidated as associated with bone marrow suppression¹⁵ and hypertension,¹⁶ respectively. The most developed (as of this writing) ALK inhibitor **1** (crizotinib, Pfizer, Figure 1), which has been tested clinically for treatment of EML4-ALK-positive NSCLC, is a MET/ALK dual inhibitor.¹⁷ On the other hand, our reported ALK inhibitor **2**¹⁸ (IC₅₀ = 1.5 nM, Figure 1) did not have potent inhibitory activity against MET (IC₅₀ = 7200 nM) but showed submicromolar IC₅₀ values against several tyrosine kinases including KDR. Therefore, further modification was performed to address this issue.

To achieve high target selectivity, on the basis of the binding mode of **2** with ALK homology models, we designed 9-substituted 6,6-dimethyl-11-oxo-6,11-dihydro-5H-benzo[*b*]carbazoles which recognize a unique amino acid sequence of ALK in the ATP binding site. For an efficient derivatization at the 9-position of 6,6-dimethyl-11-oxo-6,11-dihydro-5H-benzo[*b*]carbazole, we modified **13a** (Figure 1) as a scaffold instead of **2**, using a common intermediate. Eventually we identified the 9-ethyl derivative **13d** as a highly selective ALK inhibitor.

Herein, we wish to report the discovery of a highly selective and potent ALK inhibitor, **13d**, as well as its pharmacokinetics and in vivo efficacy.

Received: May 23, 2011

Published: August 08, 2011

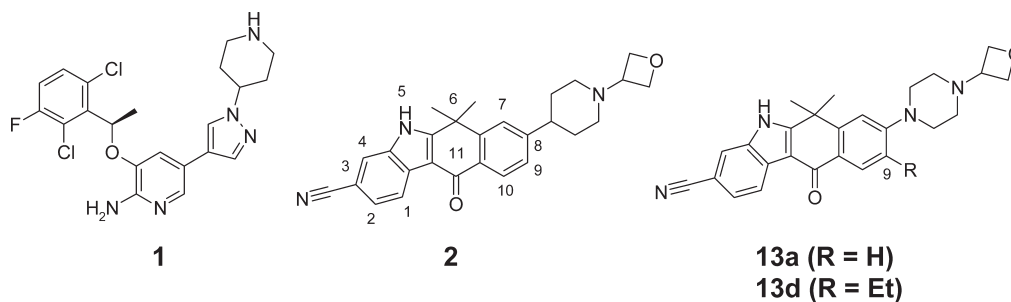
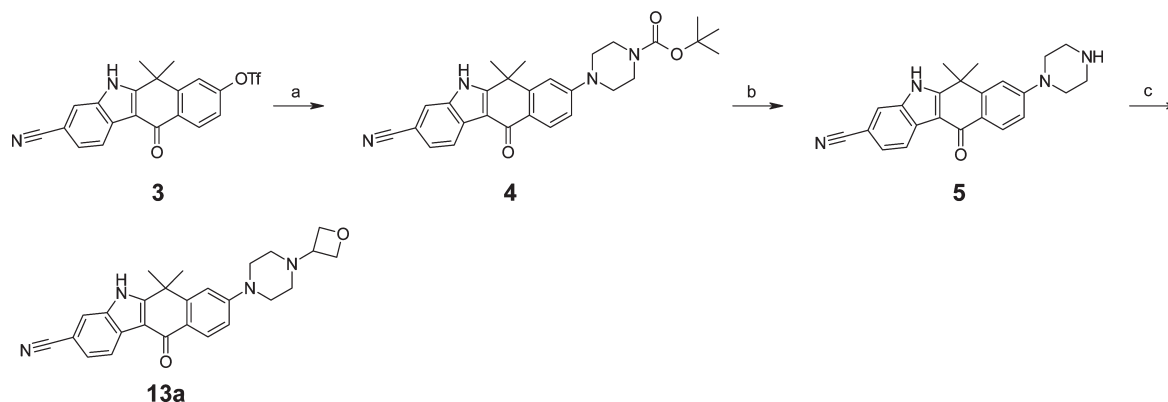


Figure 1. Structure of ALK inhibitors.

Scheme 1. Synthesis of Compound 13a^a

^a Reagents and conditions: (a) *N*-Boc-piperazine, NMP, 140 °C; (b) TFA, CH₂Cl₂, rt; (c) 3-oxetanone, NaBH(OAc)₃, THF, 40 °C.

CHEMISTRY

The preparation of compound 13a from intermediate 3^{18,19} is shown in Scheme 1. Aromatic nucleophilic substitution of 3 with *N*-Boc-piperazine gave compound 4. After removal of Boc group with trifluoroacetic acid, reductive alkylation of 5 with 3-oxetanone and sodium triacetoxyborohydride in tetrahydrofuran afforded the target compound 13a.

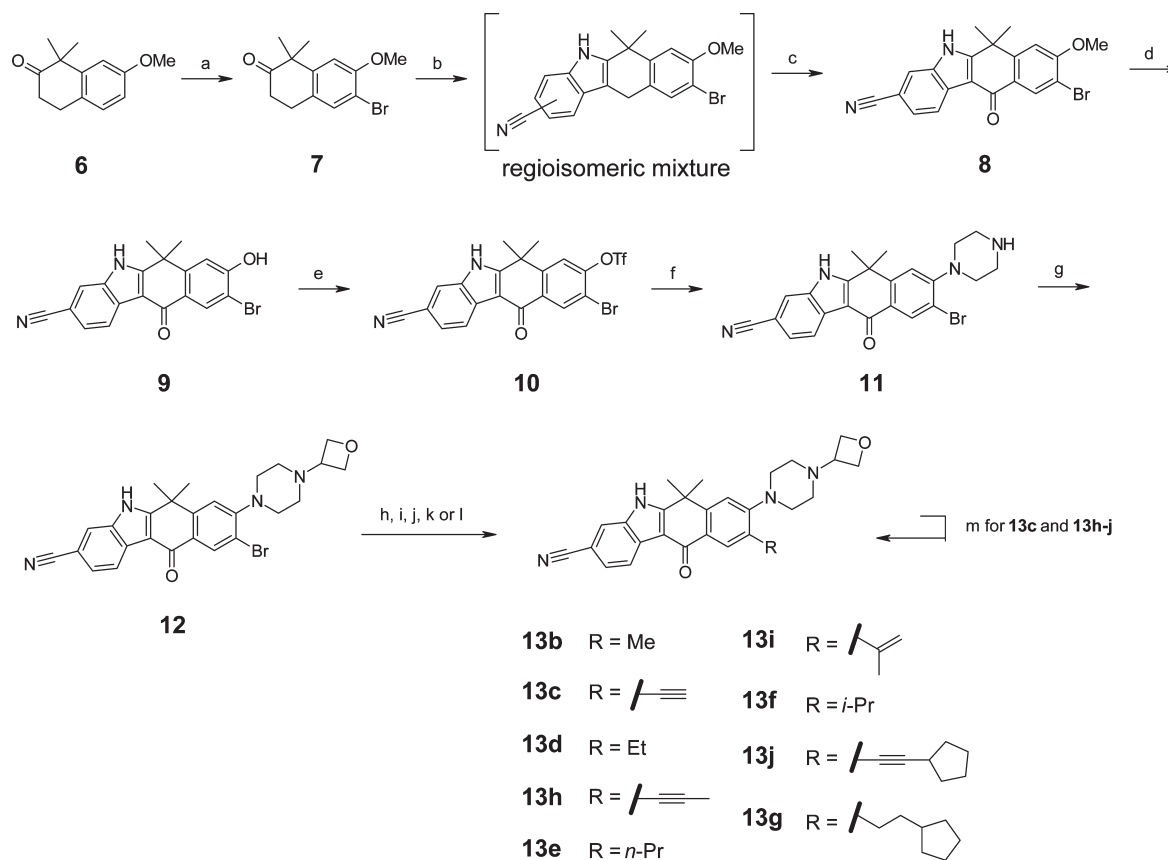
The synthesis of 8,9-substituted 6,6-dimethyl-11-oxo-6,11-dihydro-5H-benzo[b]carbazoles (13b–j) is summarized in Scheme 2. After bromination of compound 6²⁰ with *N*-bromosuccinimide, the Fischer indole ring formation of 7 gave a 1:1 mixture of regio isomers (1-CN- and 3-CN-derivatives). The undesired regio isomer (1-CN-derivative) was precipitated more easily than the desired one (3-CN-derivative) in organic solvents. Therefore, most of the undesired indole was removed by filtration. After washing with AcOEt/*n*-hexane, DDQ oxidation was conducted without further purification. Washing the resulting extract with AcOEt afforded the desired ketone 8 as a single product. A methoxy group at 8-position was converted into a triflate group by demethylation with pyridinium hydrochloride at 190 °C followed by treatment with triflic anhydride. The triflate 10 was treated with piperazine in NMP to give 8-piperazinyl compound 11. The reductive alkylation of 11 with 3-oxetanone and sodium cyanoborohydride in tetrahydrofuran/methanol afforded 12. A versatile intermediate 12 allows efficient derivatization at the 9-position. The intermediate was treated with corresponding building blocks under conventional Pd-catalyzed cross-coupling conditions to give compounds 13b, 13h, 13i, and 13j. 9-TIPS-acetylene derivative was deprotected with TBAF to give compound 13c. Hydrogenation of

13c, 13h, 13i, and 13j with catalytic palladium on charcoal afforded the corresponding 9-alkyl derivatives 13d, 13e, 13f, and 13g.

RESULTS AND DISCUSSION

Molecular Design. Since our previous study¹⁸ revealed that the ALK inhibitors bearing a 6,6-dimethyl-11-oxo-6,11-dihydro-5H-benzo[b]carbazole scaffold were ATP competitive, we investigated the amino acid sequences surrounding the ATP-binding site of several kinases. We found that the amino acid residues of the E₀ region²¹ of ALK (A₁₂₀₀ and G₁₂₀₁) were characteristically small (Chart 1) and that only 14 out of 490 kinases have the same amino acid sequence in the region as that of ALK (existence ratio is less than 3%).²² The region often serves as an entrance for ligand binding, and ALK is considered to have a wide-open surface for binding of a ligand. Therefore, we considered that the steric repulsion between a ligand and the amino acid residues of the E₀ region of off-target proteins should afford high ALK selectivity.

The docking study of 2 with our ALK homology models indicates that the 9-position of 6,6-dimethyl-11-oxo-6,11-dihydro-5H-benzo[b]carbazole scaffold would be closest to A₁₂₀₀ of the E₀ region of ALK protein. During this work, we used ALK homology models for the docking study because no ALK crystal structure was available at that time. On the basis of the binding model, we designed 9-substituted 6,6-dimethyl-11-oxo-6,11-dihydro-5H-benzo[b]carbazoles to know the influence on kinase selectivity. Because the residues of amino acids in the E₀ region of ALK are hydrophobic (A₁₂₀₀ and G₁₂₀₁), we chose several

Scheme 2. Synthesis of Compound 13b–g^a

^a Reagents and conditions: (a) *N*-bromosuccinimide, CH₃CN, rt; (b) 3-cyanophenylhydrazine, TFA, 100 °C; (c) DDQ, THF/H₂O, 0 °C; (d) pyridinium hydrochloride, 190 °C; (e) trifluoromethanesulfonic anhydride, pyridine, rt; (f) piperazine, NMP, 120 °C; (g) 3-oxetanone, NaBH₃CN, AcOH, THF/MeOH, rt; (h) trimethylboroxine, Pd(PPh₃)₄, K₂CO₃, DMF, 100 °C; (i) TIPS-acetylene, Pd(CH₃CN)₂Cl₂, X-Phos, Cs₂CO₃, CH₃CN, 80 °C, and then TBAF, THF, rt; (j) propyne, Pd(CH₃CN)₂Cl₂, X-Phos, Cs₂CO₃, CH₃CN, 80 °C; (k) isopropenylboronic acid pinacol ester, Pd(PPh₃)₂Cl₂, Na₂CO₃, DME/H₂O, 80 °C; (l) cyclopentylacetylene, Pd(CH₃CN)₂Cl₂, X-Phos, Cs₂CO₃, CH₃CN, 80 °C; (m) 10% Pd/C, H₂ gas, THF/MeOH, rt.

Chart 1. Amino Acid Sequences of ALK and Off-Target Proteins

ALK	L ₁₁₉₆	E ₁₁₉₇	L ₁₁₉₈	M ₁₁₉₉	A ₁₂₀₀	G ₁₂₀₁	G ₁₂₀₂	D ₁₂₀₃
KIT	T ₆₇₀	E ₆₇₁	Y ₆₇₂	C ₆₇₃	C ₆₇₄	Y ₆₇₅	G ₆₇₆	D ₆₇₇
KDR	V ₉₁₆	E ₉₁₇	F ₉₁₈	C ₉₁₉	K ₉₂₀	F ₉₂₁	G ₉₂₂	N ₉₂₃
MET	L ₁₁₅₇	P ₁₁₅₈	Y ₁₁₅₉	M ₁₁₆₀	K ₁₁₆₁	H ₁₁₆₂	G ₁₁₆₃	D ₁₁₆₄

Gatekeeper Hinge region E₀ region

substituents which are expected to make a hydrophobic interaction with these residues. However, the regioselective C–C bond formation of intermediate 10 at either 8- or 9-position was not successful under palladium-catalyzed cross-coupling conditions (Scheme 2). Therefore, the C–N bond was formed regioselectively at the 8-position (from 10 to 11), and an efficient derivatization at the 9-position was conducted from the common intermediate 12.

Recently, we obtained an X-ray cocrystal structure of another 6,6-dimethyl-11-oxo-6,11-dihydro-5*H*-benzo[*b*]carbazole derivative 14 (CH₅424802, Figure 2)²³ with human ALK (PDB code 3AOX). The binding model²⁴ of 13a derived from the X-ray

coordinates (Figure 2) overlapped well with that of 2 based on our ALK homology models. The result indicates that our docking study is highly reliable.

Structure–Activity Relationship (SAR). The inhibitory activity against the four kinases and against KARPAS-299 (an *NPM*-ALK-positive ALCL cell line),²⁵ and the in vitro metabolic stability are summarized in Table 1. As expected, a substituent at 9-position affected inhibitory activity against both ALK and off-target proteins. The 9-methyl group did not remarkably affect inhibitory activity against any proteins (13b). In contrast, bigger substituents than the methyl group notably weakened inhibitory activity against off-target proteins (13c–13g). These results indicate that steric bulkiness is a critical factor for inhibitory activity against off-target proteins. Among 13c–13g, inhibitory activity against ALK was inversely proportional to bulkiness of the 9-substituent. The results suggest that C2-unit (ethyl and ethynyl groups) is optimum to occupy the space of the E₀ region and would make a hydrophobic interaction with the amino acid residues there.

On metabolic stability, on the other hand, there was no impact made by a substituent at 9-position except for the most bulky derivative 13g, which showed relatively higher in vitro clearance (CL) value in mouse liver microsome in the presence of NADPH.

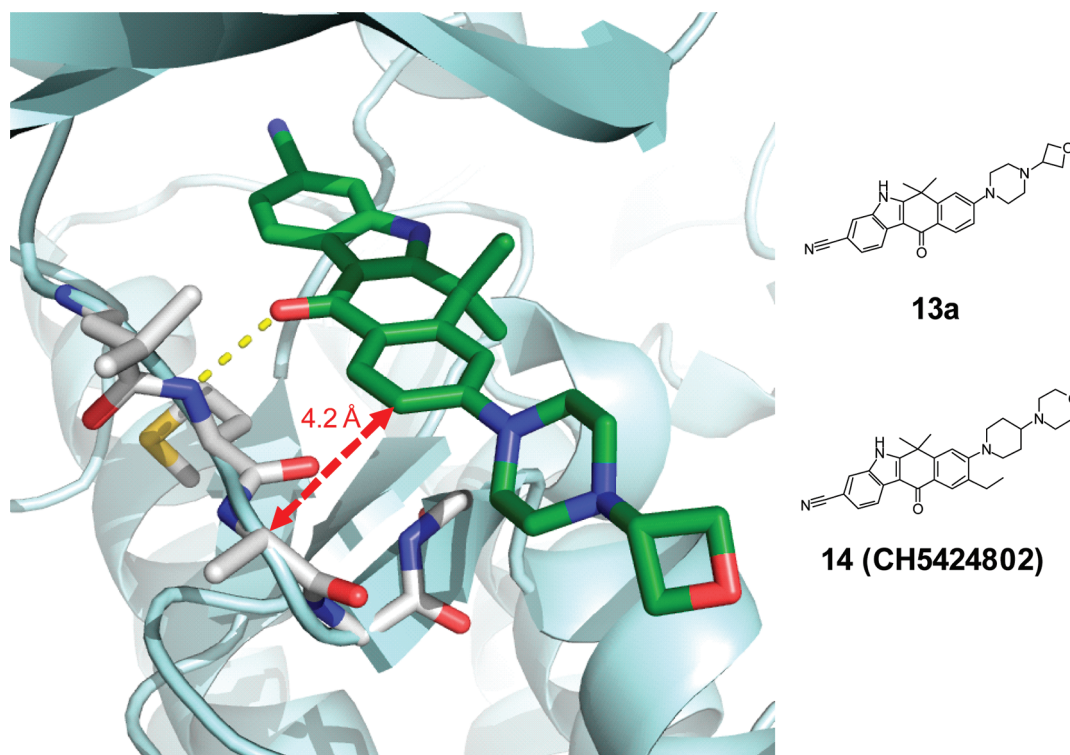


Figure 2. Binding model of **13a** in complex with human ALK derived from the X-ray cocrystal structure with **14** (PDB code 3AOX). Compound **13a** is shown as a stick model colored by element type (C in green, O in red, and N in blue). Overall structure of human ALK is shown as a cartoon diagram in pale blue. Residues L₁₁₉₈ through G₁₂₀₂ of human ALK are shown as a stick model colored by element type as the ligand except C in white and S in yellow. A hydrogen bond between the carbonyl oxygen of **13a** and the backbone amide of M₁₁₉₉ (hinge) is depicted by a yellow dashed line. Hydrogen atoms and solvent molecules are not displayed for clarity. The distance between C9 and alpha carbon of A₁₂₀₀ is 4.2 Å. The figure was prepared with PyMol (<http://www.pymol.org>).

Among the derivatives, **13d** showed both strong inhibitory activity against ALK and antiproliferative activity against KARPAS-299 with high target selectivity and favorable in vitro metabolic stability.

Kinase Selectivity Profile. Compound **13d** was further evaluated for inhibitory activity against 17 tyrosine and serine/threonine kinases (Table 2). Compound **13d** showed improved target selectivity compared to that of our first generation ALK inhibitor **2**. The amino acid sequences in the E₀ region of 17 kinases support our hypothesis. It is noteworthy that **13d** showed a relatively low IC₅₀ value against INSR and that the kinase has the same amino acid in a corresponding position to that of A₁₂₀₀ in ALK. This fact indicates that A₁₂₀₀ would be a key amino acid for kinase selectivity.

Pharmacokinetics. The pharmacokinetic properties of **13d** were evaluated in monkeys (Table 3). Compound **13d** demonstrated favorable plasma clearance in monkeys, which is consistent with in vitro CL values in human and mouse liver microsomes in the presence of NADPH. In addition, **13d** showed moderate bioavailability and T_{1/2} value. A preliminary pharmacokinetic study was conducted in mice. The result is provided in Supporting Information.

Efficacy in Tumor Xenograft Studies. Compound **13d** was also evaluated in an established NPM-ALK-positive ALCL xenograft model in mice (Figure 3). Mice bearing KARPAS-299 were administered **13d** orally once daily for 11 days at 2, 6, and 20 mg/kg, their body weight and the volume of the tumor were measured twice a week, and the relative body weight was

calculated. Compound **13d** showed strong antitumor efficacy dose-dependently. A significant tumor regression (TGI = 119%) was observed at the dose of 20 mg/kg without apparent body weight loss. This efficacy is greater than that of the first generation ALK inhibitor **2**.¹⁸

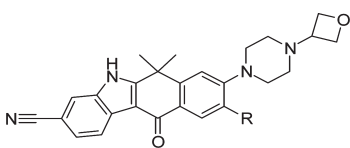
CONCLUSION


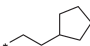
By modifying our previously reported ALK inhibitor **2** bearing a unique 6,6-dimethyl-11-oxo-6,11-dihydro-5H-benzo-[b]carbazole scaffold, we identified highly selective ALK inhibitors which eliminate the concerns of adverse events caused by off-target kinase modulation. Among them, highly selective and potent ALK inhibitor **13d**, bearing an ethyl group at the 9-position, was discovered. The location of the ethyl group around the E₀ region at the binding sites of kinases might have afforded high ALK selectivity over off-target kinases. Compound **13d** showed inhibitory activity against ALK with an IC₅₀ value of 2.9 nM and antiproliferative activity against KARPAS-299 with an IC₅₀ value of 12.8 nM. The pharmacokinetic properties of **13d** were favorable. Oral administration of **13d** at 20 mg/kg demonstrated significant tumor regression (TGI = 119%) without body weight loss in an established NPM-ALK-positive ALCL xenograft model in mice.

EXPERIMENTAL SECTION

Chemistry. All solvents and reagents were obtained commercially. ¹H and ¹³C NMR spectra were recorded on a VARIAN 400-MR or a

Table 1. In Vitro Inhibitory Activity and Metabolic Stability of 9-Substituted Derivatives



Compd	R	IC ₅₀ (nM)					CL (μL/min/mg)	
		ALK ^a	KDR ^a	KIT ^a	MET ^a	KARPAS-299	human	mouse
13a	H	27.0	137	83.9	>5000	47.9	9.6	15.1
13b	Me	10.6	60.8	49.8	>5000	14.8	22.6	7.0
13c		2.7	455	2422	>5000	4.2	18.9	2.1
13d	Et	2.9	>5000	>5000	>5000	12.8	17.0	4.5
13e	<i>n</i> -Pr	15.1	>5000	>5000	>5000	25.3	19.4	4.7
13f	<i>i</i> -Pr	66.4	>5000	>5000	>5000	118	17.4	4.1
13g		186	>5000	>5000	>5000	544	17.8	44.7

^a The values are averages of 2 separate determinations. The values in each assay are provided in Supporting Information.

Table 2. Inhibitory Activity of 2 and 13d against 17 Kinases, and Amino Acids in the E₀ Region^a

	Enzyme	IC ₅₀ (μM)		E ₀ region	
		2	13d		
Tyrosine kinase	ALK	0.0015	0.0029	A	G
	INSR	0.31	0.46	A	H
	KDR	0.10	>50	K	F
	SRC	0.25	>50	S	K
	FGFR2	0.36	>50	S	K
	ABL	0.37	>50	T	Y
	IGF1R	1.00	>50	T	R
	MET	7.20	>50	K	H
	EGFR	>50	>50	P	F
	KIT	>50	>50	C	Y
	HER2	>50	>50	P	Y
Serine/threonine kinase	AKT1	>50	>50	N	G
	Aurora A	>50	>50	P	L
	PKCa	>50	>50	N	G
	PKCb1	>50	>50	N	G
	PKCb2	>50	>50	N	G
	Raf-1	>50	>50	E	G

^a The experimental details for each kinase are available in Supporting Information.

JEOL JNM-EX270 spectrometer, and chemical shifts are expressed as δ units using tetramethylsilane as an internal standard. The spectral splitting patterns are described as follows: s, singlet; d, doublet; dd, double doublet; t, triplet; q, quartet; m, multiplet; and bs, broad singlet peak. Liquid chromatography/mass spectra (LCMS) were measured by

a Waters LCMS system with a SunFire C18 (5 μm, 4.6 mm × 50 mm) column or a Wakosil-II 3C18 AR (3.0–3.7 μm, 4.6 mm × 30 mm) column (mobile phase, CH₃CN/H₂O with 0.05% TFA; flow rate, 2.0 mL/min). High resolution mass spectra (HRMS) were measured with a Thermo Fisher Scientific LTQ Orbitrap XL MS spectrometer using an ESI source coupled to a Waters HPLC system operating in reversed phase with an ACQUITY UPLC BEH C18 (1.7 μm, 2.1 mm × 50 mm) column. Flash column chromatography was performed with Biotage SNAP cartridges or SILICYCLE SiliaSep packed columns. Preparative HPLC was conducted with a SunFire Prep C18 OBD (5 μm, 30 mm × 50 mm) column (mobile phase, CH₃CN/H₂O with 0.05% TFA). All tested compounds are ≥95% except for 13e (93%). The purity was determined by LCMS analysis.

6,6-Dimethyl-8-(1-oxetan-3-yl-piperidin-4-yl)-11-oxo-6,11-dihydro-5H-benzo[b]carbazole-3-carbonitrile (**2**). The synthetic procedure of **2** was described in a previous report.¹⁸ LCMS (ESI), >95% pure; *m/z*, 426 [M + H]⁺. ¹H NMR (400 MHz, DMSO-*d*₆) δ 12.74 (1H, bs), 8.32 (1H, d, *J* = 8.4 Hz), 8.13 (1H, d, *J* = 7.9 Hz), 8.00 (1H, s), 7.74 (1H, s), 7.61 (1H, d, *J* = 7.9 Hz), 7.40 (1H, d, *J* = 8.4 Hz), 4.56 (2H, t, *J* = 6.4 Hz), 4.46 (2H, t, *J* = 6.1 Hz), 3.46–3.39 (1H, m), 2.85–2.82 (2H, m), 2.71–2.64 (1H, m), 1.92–1.86 (2H, m), 1.82–1.79 (4H, m), 1.77 (6H, s). ¹³C NMR (100 MHz, DMSO-*d*₆) δ 179.0, 160.1, 150.9, 148.1, 135.6, 129.3, 127.5, 125.7, 125.3, 125.0, 124.7, 121.5, 119.9, 116.3, 109.2, 104.5, 74.6, 58.5, 49.8, 41.9, 36.5, 32.2, 29.7. HRMS (ESI), *m/z* calcd for C₂₇H₂₈N₃O₂ [M + H]⁺ 426.2176, found 426.2179.

4-(3-Cyano-6,6-dimethyl-11-oxo-6,11-dihydro-5H-benzo[b]carbazol-8-yl)-piperazine-1-carboxylic Acid *tert*-Butyl Ester (**4**). To a solution of **3**¹⁸ (25 mg, 0.058 mmol) in NMP (1.25 mL) was added *N*-Boc-piperazine (302 mg, 28 equiv). After stirring for 27 h at 140 °C, the reaction mixture was purified by preparative HPLC to give **4** (15 mg,

Table 3. Pharmacokinetic Profiles of 13d in Monkeys (Male and Female)^a

	<i>F</i> ^b (%)	po			iv		
		AUC (ng·h/mL)	<i>C</i> _{max} (ng/mL)	<i>T</i> _{1/2} (h)	CL _{tot} (mL/min/kg)	<i>V</i> _{dss} (L/kg)	<i>T</i> _{1/2} (h)
no. 1	21.6	2510	288	6.27	0.808	0.298	4.6
no. 2	34.7	4030	366	6.22	0.652	0.294	5.9
mean	28.2	3270	327	6.25	0.730	0.296	5.3

^aDose: po and iv at 0.5 mg/kg (*n* = 2). ^bOral bioavailability.

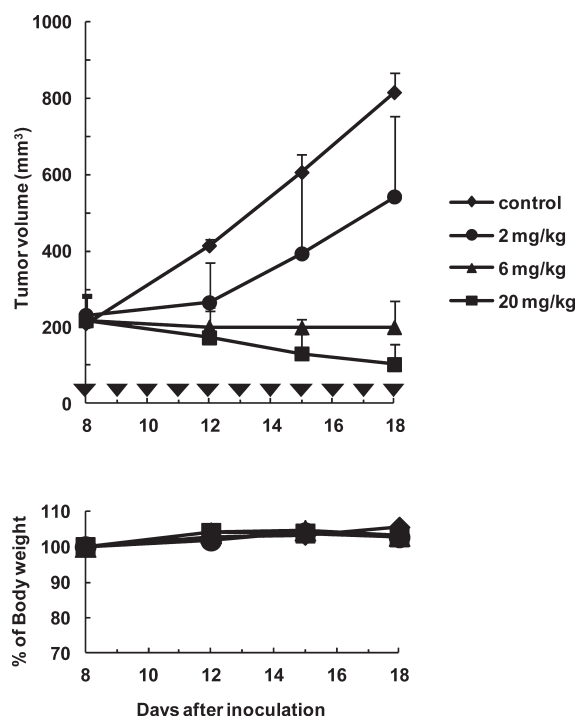


Figure 3. Growth inhibitory effect of 13d on KARPAS-299 tumor growth in mouse xenograft model. SCID mice bearing KARPAS-299 were administered compound 13d orally once daily for 11 d (days 8–18) at 2 mg/kg (tumor growth inhibition TGI = 49%), 6 mg/kg (TGI = 103%), and 20 mg/kg (TGI = 119%).

55%). ¹H NMR (270 MHz, CDCl₃) δ 8.52 (1H, d, *J* = 8.1 Hz), 8.32 (1H, d, *J* = 9.7 Hz), 7.72 (1H, s), 7.53 (1H, d, *J* = 8.1 Hz), 6.94–7.03 (2H, m), 3.59–3.67 (4H, m), 3.32–3.42 (4H, m), 1.50 (9H, s). MS (ESI) *m/z*: 471 [M + H]⁺.

6,6-Dimethyl-11-oxo-8-piperazin-1-yl-6,11-dihydro-5H-benzo[b]carbazole-3-carbonitrile (**5**). To a solution of **4** (15 mg, 0.032 mmol) in CH₂Cl₂ (2.0 mL) was added trifluoroacetic acid (0.4 mL, excess amount). After stirring for 2 h at room temperature, the reaction mixture was evaporated under reduced pressure. The residue was purified by preparative HPLC to give **5** as a light-yellow powder (10 mg, 89%). ¹H NMR (400 MHz, DMSO-*d*₆) δ: 8.32 (1H, d, *J* = 8.5 Hz), 8.03 (1H, d, *J* = 9.1 Hz), 7.99 (1H, s), 7.59 (1H, dd, *J* = 8.2, 1.5 Hz), 7.20 (1H, d, *J* = 2.4 Hz), 7.04 (1H, dd, *J* = 8.8, 2.1 Hz), 3.30–3.32 (4H, m), 2.87–2.88 (4H, m), 1.77 (6H, s). MS (ESI) *m/z*: 371 [M + H]⁺.

6,6-Dimethyl-8-(4-oxetan-3-yl-piperazin-1-yl)-11-oxo-6,11-dihydro-5H-benzo[b]carbazole-3-carbonitrile (**13a**). To a solution of **5** (26 mg, 0.07 mmol) in THF (2.0 mL) were added 3-oxetanone (15 mg, 3 equiv) and sodium triacetoxyborohydride (59 mL, 4 equiv). After stirring for 7 h at 40 °C, the reaction mixture was cooled to room temperature and evaporated under reduced pressure. The residue was dissolved with

AcOEt. After addition of water, stirring of the resulting solution for 0.5 h at 0 °C afforded a precipitate. The precipitate was filtered off and washed with AcOEt/water to give **13a** as a light-yellow solid (27 mg, 90%). LCMS (ESI), >95% pure; *m/z*, 427 [M + H]⁺. ¹H NMR (400 MHz, DMSO-*d*₆) δ 8.29 (1H, dd, *J* = 8.2, 0.59 Hz), 8.02 (1H, d, *J* = 9.0 Hz), 7.97 (1H, d, *J* = 0.59 Hz), 7.56 (1H, dd, *J* = 8.0, 1.4 Hz), 7.22 (1H, d, *J* = 2.3 Hz), 7.04 (1H, dd, *J* = 8.8, 2.2 Hz), 4.56–4.59 (2H, m), 4.47–4.50 (2H, m), 3.43–3.48 (1H, m), 3.39–3.42 (4H, m), 2.40–2.42 (4H, m), 1.74 (6H, s).

6-Bromo-7-methoxy-1,1-dimethyl-3,4-dihydro-1H-naphthalen-2-one (**7**). To a solution of **6**²⁰ (2.00 g, 9.79 mmol) in CH₃CN (40 mL) was added *N*-bromosuccinimide (1.92 g, 1.1 equiv). After stirring for 2.5 h at room temperature, the reaction mixture was poured into water (40 mL) to give a white precipitate. This was collected by filtration and air-dried to give **7** (2.55 g, 92%). ¹H NMR (400 MHz, DMSO-*d*₆) δ: 7.43 (1H, s), 7.04 (1H, s), 3.87 (3H, s), 2.98 (2H, t, *J* = 6.8 Hz), 2.59 (2H, t, *J* = 6.8 Hz), 1.34 (6H, s). HRMS (ESI), *m/z* calcd for C₁₃H₁₆O₂Br [M + H]⁺ 283.0328, found 283.0333.

9-Bromo-8-methoxy-6,6-dimethyl-11-oxo-6,11-dihydro-5H-benzo[b]carbazole-3-carbonitrile (**8**). A mixture of **7** (7.89 g, 27.8 mmol), 3-cyanophenylhydrazine (4.45 g, 1.2 equiv), and trifluoroacetic acid (250 mL) was heated at 100 °C for 2 h. The reaction mixture was cooled and then evaporated under reduced pressure. The residue was neutralized by saturated aqueous NaHCO₃ and extracted with AcOEt. The combined organic layers were washed with brine, and precipitated solid (undesired regioisomer) was filtered off. The filtrate was evaporated under reduced pressure. The resulting solid was washed with AcOEt/*n*-hexane to give the desired compound roughly purified, which was used in the next reaction without further purification. To a solution of the compound in THF (120 mL) and water (12 mL) was gradually added DDQ (4.55 g, excess amount). After stirring for 3 h at 0 °C, the reaction mixture was evaporated under reduced pressure. The residue was dissolved with CPME. The solution was washed with aqueous NaOH, water, and brine, dried over MgSO₄, filtered, and concentrated under reduced pressure. The residue was washed with AcOEt to yield **8** (1.90 g, 17% in two steps from **7**). ¹H NMR (400 MHz, DMSO-*d*₆) δ 12.82 (1H, s), 8.28–8.32 (2H, m), 8.03 (1H, s), 7.61 (1H, d, *J* = 8.4 Hz), 7.49 (1H, s), 4.04 (3H, s), 1.81 (6H, s). HRMS (ESI), *m/z* calcd for C₂₀H₁₆BrN₂O₂ [M + H]⁺ 395.039, found 395.0392.

9-Bromo-8-hydroxy-6,6-dimethyl-11-oxo-6,11-dihydro-5H-benzo[b]carbazole-3-carbonitrile (**9**). A mixture of **8** (270 mg, 0.68 mmol) and pyridinium hydrochloride (1.62 g, 22 equiv) was heated to 190 °C in the microwave for 1.5 h. The reaction mixture was dissolved in water, neutralized by saturated aqueous NaHCO₃, and extracted with AcOEt/THF (×3). The combined organic layer was washed with aqueous NaHCO₃ and brine, dried over MgSO₄, filtered, and concentrated under reduced pressure. The residue was purified by flash column chromatography (*n*-hexane/AcOEt) to yield **9** as a brown solid (140 mg, 54%). ¹H NMR (400 MHz, DMSO-*d*₆) δ 12.77 (1H, s), 11.13 (1H, s), 8.31 (1H, d, *J* = 7.9 Hz), 8.25 (1H, s), 8.01 (1H, s), 7.61 (1H, d, *J* = 7.9 Hz), 7.28 (1H, s), 1.74 (6H, s). HRMS (ESI), *m/z* calcd for C₁₉H₁₄BrN₂O₂ [M + H]⁺ 381.0233, found 381.0239.

Trifluoromethanesulfonic Acid 9-Bromo-3-cyano-6,6-dimethyl-11-oxo-6,11-dihydro-5H-benzo[b]carbazol-8-yl Ester (**10**). To a solution of **9** (140 mg, 0.37 mmol) in pyridine (2 mL) was added trifluoromethanesulfonic anhydride (188 μ L, 3 equiv) at 0 °C. After stirring for 1.5 h at room temperature, the reaction mixture was poured into aqueous NH₄Cl and then extracted with AcOEt (\times 2). The combined organic layer was washed with brine, dried over Na₂SO₄, filtered, and concentrated under reduced pressure. The residue was purified by flash column chromatography (*n*-hexane/AcOEt) to yield **10** as an off-white solid (120 mg, 64%). ¹H NMR (400 MHz, DMSO-*d*₆) δ 12.99 (1H, s), 8.51 (1H, s), 8.31 (1H, d, *J* = 8.2 Hz), 8.17 (1H, s), 8.07 (1H, s), 7.67 (1H, d, *J* = 8.2 Hz), 1.81 (6H, s). HRMS (ESI), *m/z* calcd for C₂₀H₁₃BrF₃N₂O₄S [M + H]⁺ 512.9726, found 512.9728.

9-Bromo-6,6-dimethyl-11-oxo-8-piperazin-1-yl-6,11-dihydro-5H-benzo[b]carbazole-3-carbonitrile (**11**). To a solution of **10** (6.0 g, 11.7 mmol) in NMP (75 mL) was added piperazine (10.1 g, 10 equiv). After stirring for 30 min at 120 °C, the reaction mixture was cooled and poured into water to afford precipitation. The precipitate was filtered off and dried under reduced pressure to yield **11** as a white solid (3.9 g, 74%). ¹H NMR (400 MHz, DMSO-*d*₆) δ 8.30 (1H, d, *J* = 7.9 Hz), 8.28 (1H, s), 8.00 (1H, s), 7.61 (1H, d, *J* = 7.9 Hz), 7.41 (1H, s), 3.32 (2H, bs), 3.01–3.10 (4H, m), 2.85–2.91 (4H, m), 1.76 (6H, s). HRMS (ESI), *m/z* calcd for C₂₃H₂₂BrN₄O [M + H]⁺ 449.0972, found 449.0973.

9-Bromo-8-(4-cyclopropyl-piperazin-1-yl)-6,6-dimethyl-11-oxo-6,11-dihydro-5H-benzo[b]carbazole-3-carbonitrile (**12**). To a solution of **11** (50 mg, 0.11 mmol) in MeOH/THF/AcOH (1.5 mL/1.5 mL/0.25 mL) were added 3-oxetanone (39.4 μ L, 7 equiv) and sodium cyanoborohydride (36.8 mg, 5 equiv). To the mixture, an excess amount of 3-oxetanone (total 25 equiv) was added gradually at room temperature. The reaction was monitored by HPLC until the starting material was consumed (stirred for 24 h). The resulting reaction mixture was poured into water to give a precipitate. The precipitated solid was filtered off and washed with water to afford **12** as an off-white solid (41.2 mg, 73%). ¹H NMR (400 MHz, DMSO-*d*₆) δ 12.83 (1H, s), 8.30 (1H, d, *J* = 7.9 Hz), 8.28 (1H, s), 8.02 (1H, s), 7.62 (1H, d, *J* = 7.9 Hz), 7.48 (1H, s), 4.56–4.61 (2H, m), 4.46–4.51 (2H, m), 3.47–3.56 (1H, m), 3.15–3.24 (4H, m), 2.44–2.54 (4H, m), 1.78 (6H, s). HRMS (ESI), *m/z* calcd for C₂₆H₂₆BrN₄O₂ [M + H]⁺ 505.1234, found 505.1235.

6,6,9-Trimethyl-8-(4-oxetan-3-yl-piperazin-1-yl)-11-oxo-6,11-dihydro-5H-benzo[b]carbazole-3-carbonitrile (**13b**). A mixture of **12** (30 mg, 0.06 mmol), trimethylboroxine (16.5 μ L, 2 equiv), potassium carbonate (24.6 mg, 3 equiv), DMF (0.9 mL), and Pd(PPh₃)₄ (6.86 mg, 0.1 equiv) was stirred for 10 h at 100 °C. The reaction mixture was then cooled, diluted with AcOEt, washed with brine, dried over Na₂SO₄, filtered, and concentrated under reduced pressure. The residue was purified by preparative HPLC to give **13b** (11.2 mg, 42%). LCMS (ESI), >95% pure; *m/z*, 441 [M + H]⁺. ¹H NMR (270 MHz, DMSO-*d*₆) δ 12.71 (1H, s), 8.32 (1H, d, *J* = 8.1 Hz), 8.01 (1H, s), 7.97 (1H, s), 7.60 (1H, d, *J* = 8.1 Hz), 7.32 (1H, s), 4.57–4.61 (2H, m), 4.47–4.51 (2H, m), 3.49–3.55 (1H, m), 2.99–3.11 (4H, m), 2.42–2.50 (4H, m), 2.33 (3H, s), 1.76 (6H, s).

9-Ethynyl-6,6-dimethyl-8-(4-oxetan-3-yl-piperazin-1-yl)-11-oxo-6,11-dihydro-5H-benzo[b]carbazole-3-carbonitrile (**13c**). A mixture of **12** (26.7 mg, 0.05 mmol), TIPS-acetylene (17.8 μ L, 1.5 equiv), cesium carbonate (81.5 mg, 4.5 equiv), X-Phos (7.56 mg, 0.3 equiv), CH₃CN (1.0 mL), and Pd(CH₃CN)₂Cl₂ (1.37 mg, 0.1 equiv) was stirred for 4 h at 80 °C. The reaction mixture was then cooled, diluted with AcOEt, washed with brine, dried over Na₂SO₄, filtered, and concentrated under reduced pressure. The residue was used in the next reaction without further purification. To a solution of the residue in THF (2.0 mL) was added TBAF (74.2 μ L, 1.5 equiv). After stirring for 1 h at room temperature, the reaction mixture was diluted with AcOEt, washed with water (\times 6) and brine, dried over Na₂SO₄, filtered, and concentrated

under reduced pressure. The residue was triturated with MeOH (1.0 mL). The precipitated solid was filtered off and washed with *n*-hexane to afford **13c** as a brown solid (10.7 mg, 48%). LCMS (ESI), 95% pure; *m/z* 451 [M + H]⁺. ¹H NMR (400 MHz, DMSO-*d*₆) δ : 12.77 (1H, s), 8.31 (1H, d, *J* = 7.9 Hz), 8.16 (1H, s), 8.02 (1H, s), 7.61 (1H, d, *J* = 7.9 Hz), 7.27 (1H, s), 4.55–4.63 (2H, m), 4.46–4.53 (3H, m), 3.47–3.56 (1H, m), 3.35–3.43 (4H, m), 2.43–2.50 (4H, m), 1.78 (6H, s). HRMS (ESI), *m/z* calcd for C₂₈H₂₇N₄O₂ [M + H]⁺ 451.2129, found 451.2127.

9-Ethyl-6,6-dimethyl-8-(4-oxetan-3-yl-piperazin-1-yl)-11-oxo-6,11-dihydro-5H-benzo[b]carbazole-3-carbonitrile (**13d**). To a solution of **13c** (34.0 mg, 0.08 mmol) in MeOH/THF (1.6 mL/2.4 mL), 10% palladium on charcoal (20 mg, 60% w/w) was added at room temperature. After being stirred vigorously under hydrogen gas for 2 h at room temperature, the reaction mixture was filtered through Celite. The filtrate was concentrated under reduced pressure. The residue was purified by flash column chromatography (CH₂Cl₂/MeOH) to yield **13d** as a white solid (6.9 mg, 19%). LCMS (ESI), 95% pure; *m/z* 455 [M + H]⁺. ¹H NMR (400 MHz, DMSO-*d*₆) δ 12.70 (1H, s), 8.29 (1H, d, *J* = 8.4 Hz), 8.05 (1H, s), 8.00 (1H, s), 7.61 (1H, d, *J* = 8.4 Hz), 7.38 (1H, s), 4.55–4.62 (2H, m), 4.45–4.52 (2H, m), 3.48–3.55 (1H, m), 2.98–3.05 (4H, m), 2.71 (2H, q, *J* = 7.5 Hz), 2.43–2.51 (4H, m), 1.74 (6H, s), 1.26 (3H, t, *J* = 7.5 Hz). ¹³C NMR (100 MHz, DMSO-*d*₆) δ 179.1, 159.9, 155.0, 146.8, 136.5, 135.8, 127.8, 126.4, 126.0, 124.5, 121.6, 119.9, 116.7, 116.2, 109.5, 104.7, 74.3, 58.6, 51.5, 49.4, 36.6, 30.1, 22.7, 14.5. HRMS (ESI), *m/z* calcd for C₂₈H₃₁N₄O₂ [M + H]⁺ 455.2442, found 455.2440.

6,6-Dimethyl-8-(4-oxetan-3-yl-piperazin-1-yl)-11-oxo-9-prop-1-ynyl-6,11-dihydro-5H-benzo[b]carbazole-3-carbonitrile (**13h**). A mixture of **12** (210 mg, 0.42 mmol), cesium carbonate (609 mg, 4.5 equiv), X-Phos (29.7 mg, 0.15 equiv), CH₃CN (8.0 mL), and Pd(CH₃CN)₂Cl₂ (5.39 mg, 0.05 equiv) was stirred under propyne gas for 16 h at 80 °C. The reaction mixture was cooled and then triturated with water (12 mL). The precipitated solid was filtered off and washed with AcOEt/*n*-hexane to yield **13h** as a brown solid (153 mg, 79%). ¹H NMR (400 MHz, CD₃OD) δ 8.37 (1H, d, *J* = 8.2 Hz), 8.18 (1H, s), 7.84 (1H, s), 7.53 (1H, d, *J* = 8.2 Hz), 7.19 (1H, s), 4.70–4.77 (2H, m), 4.62–4.68 (2H, m), 3.57–3.63 (1H, m), 3.38–3.45 (4H, m), 2.54–2.61 (4H, m), 2.10 (3H, s), 1.79 (6H, s). MS (ESI) *m/z*: 465 [M + H]⁺.

6,6-Dimethyl-8-(4-oxetan-3-yl-piperazin-1-yl)-11-oxo-9-propyl-6,11-dihydro-5H-benzo[b]carbazole-3-carbonitrile (**13e**). Compound **13e** was prepared from **13h** following the same procedure as described for **13d** (48%, an off-white solid). LCMS (ESI), 93% pure; *m/z* 469 [M + H]⁺. ¹H NMR (270 MHz, DMSO-*d*₆) δ 12.75 (1H, s), 8.30 (1H, d, *J* = 8.2 Hz), 7.97–8.01 (2H, m), 7.59 (1H, d, *J* = 8.2 Hz), 7.38 (1H, s), 4.53–4.61 (2H, m), 4.43–4.51 (2H, m), 3.49–3.55 (1H, m), 2.96–3.02 (4H, m), 2.63 (2H, t, *J* = 7.3 Hz), 2.41–2.47 (4H, m), 1.73 (6H, s), 1.61–1.70 (2H, m), 0.94 (3H, t, *J* = 7.4 Hz).

9-Isopropenyl-6,6-dimethyl-8-(4-oxetan-3-yl-piperazin-1-yl)-11-oxo-6,11-dihydro-5H-benzo[b]carbazole-3-carbonitrile (**13i**). A mixture of **12** (56 mg, 0.11 mmol), isopropenylboronic acid pinacol ester (29.3 μ L, 1.4 equiv), sodium carbonate (35.2 mg, 3 equiv), DME/water (2.5 mL/0.5 mL), and Pd(PPh₃)₂Cl₂ (3.88 mg, 0.05 equiv) was stirred for 38 h at 80 °C. The reaction mixture was cooled and then triturated with water (9.0 mL). The precipitated solid was filtered off and purified by flash column chromatography (CH₂Cl₂/MeOH) to yield **13i** as a white solid (19.0 mg, 37%). ¹H NMR (270 MHz, CD₃OD + CDCl₃) δ 8.44 (1H, d, *J* = 7.8 Hz), 8.09 (1H, s), 7.83 (1H, s), 7.54 (1H, d, *J* = 7.8 Hz), 7.18 (1H, s), 5.20–5.24 (2H, m), 4.68–4.81 (4H, m), 3.56–3.70 (1H, m), 3.24–3.34 (4H, m), 2.52–2.61 (4H, m), 2.21 (3H, s), 1.82 (6H, s). MS (ESI) *m/z*: 467 [M + H]⁺.

9-Isopropyl-6,6-dimethyl-8-(4-oxetan-3-yl-piperazin-1-yl)-11-oxo-6,11-dihydro-5H-benzo[b]carbazole-3-carbonitrile (**13f**). Compound **13f** was prepared from **13i** following the same procedure as described for

13d (38%, a white solid). LCMS (ESI), >95% pure; m/z 469 $[M + H]^+$. 1H NMR (270 MHz, $CD_3OD + CDCl_3$) δ 8.44 (1H, d, $J = 7.8$ Hz), 8.27 (1H, s), 7.84 (1H, s), 7.54 (1H, d, $J = 7.8$ Hz), 7.36 (1H, s), 4.70–4.82 (4H, m), 3.63–3.73 (1H, m), 3.35–3.52 (1H, m), 3.09–3.13 (4H, m), 2.55–2.72 (4H, m), 1.81 (6H, s), 1.31 (6H, d, $J = 7.0$ Hz).

9-Cyclopentylethynyl-6,6-dimethyl-8-(4-oxetan-3-yl-piperazin-1-yl)-11-oxo-6,11-dihydro-5H-benzo[b]carbazole-3-carbonitrile (**13j**). A mixture of **12** (38 mg, 0.08 mmol), cyclopentylacetylene (26 μ L, 3 equiv), cesium carbonate (97.9 mg, 4 equiv), X-Phos (5.37 mg, 0.15 equiv), CH_3CN (2.0 mL), and $Pd(CH_3CN)_2Cl_2$ (0.97 mg, 0.05 equiv) was stirred for 14 h at 80 °C. The reaction mixture was cooled and then triturated with water (2.0 mL). The precipitated solid was filtered off and washed with *n*-hexane to yield **13j** as a light-brown solid (25 mg, 66%). 1H NMR (400 MHz, $DMSO-d_6$) δ 12.74 (1H, s), 8.31 (1H, d, $J = 8.4$ Hz), 8.04 (1H, s), 8.00 (1H, s), 7.60 (1H, d, $J = 8.4$ Hz), 7.22 (1H, s), 4.54–4.63 (2H, m), 4.43–4.53 (2H, m), 3.45–3.53 (1H, m), 3.34–3.43 (4H, m), 2.89–2.98 (1H, m), 2.41–2.50 (4H, m), 1.92–2.05 (2H, m), 1.76 (6H, s), 1.51–1.81 (6H, m). MS (ESI) m/z : 519 $[M + H]^+$.

9-(2-Cyclopentyl-ethyl)-6,6-dimethyl-8-(4-oxetan-3-yl-piperazin-1-yl)-11-oxo-6,11-dihydro-5H-benzo[b]carbazole-3-carbonitrile (**13g**). Compound **13g** was prepared from **13j** following the same procedure as described for **13d** (29%, a white solid). LCMS (ESI), >95% pure; m/z 523 $[M + H]^+$. 1H NMR (270 MHz, CD_3OD) δ 8.40 (1H, d, $J = 7.8$ Hz), 8.13 (1H, s), 7.86 (1H, s), 7.55 (1H, d, $J = 7.8$ Hz), 7.40 (1H, s), 4.62–4.78 (4H, m), 3.52–3.68 (1H, m), 3.07–3.11 (4H, m), 2.72–2.78 (2H, m), 2.56–2.60 (4H, m), 1.80 (6H, s), 1.20–1.90 (11H, m).

In Vitro Kinase Enzyme Assay. ALK protein was purchased from Carna Biosciences. The inhibitory ability was evaluated by examining their ability to phosphorylate substrate peptide (Biotin-EGPWLEEEEEE-AYGWMDF) in the presence of 30 μ M ATP and 10 mM $MgCl_2$ using time-resolved fluorescence resonance energy transfer (TR-FRET) assay. The inhibitory activity against Raf-1 was evaluated by examining the ability of the kinase to phosphorylate MEK1/2 using europium-antiphospho-MEK1/2 (Ser217/221) antibody. The quantity of enzyme and ATP and the kind of substrate and cation species added in each assay for evaluation of other kinases are given in the Supporting Information.

In Vitro Cell Growth Assay. KARPAS-299 cells were treated with various concentrations of assay compounds for 96 h. Cell growth inhibition was determined by Cell Counting Kit-8 assay.

In Vivo Antitumor Activity on KARPAS-299 in SCID Mice. Cell line (KARPAS-299) was used to evaluate antitumor activity of **13d** in vivo. It was grown as sc tumors in SCID mice (CLEA Japan, Inc.). Therapeutic experiments were started (day 0) when the tumor reached around 200 mm³. Mice (four mice per group) were randomized to treatment groups to receive vehicle or **13d** (oral, QD) on days 0 to 10. Final concentration of vehicle was 10% DMSO, 10% Cremophor EL, 15% PEG400, and 15% HPCD (2-hydroxypropyl- β -cyclodextrin). Compound **13d** was given to mice by forced oral administration using a sonde tube. The length (*L*) and width (*W*) of the tumor mass were measured, and the tumor volume (TV) was calculated as: $TV = (L \times W^2)/2$. Body weight change rate (BW) was calculated using the following formula: $BW = W/W_0 \times 100$, where *W* and *W*₀ are the body weight on a specific experimental day and on the first day of treatment, respectively. Tumor growth inhibition (TGI) was calculated using the following formula: $TGI = [1 - (T - T_0)/(C - C_0)] \times 100$, where *T* and *T*₀ are the mean tumor volumes on a specific experimental day and on the first day of treatment, respectively, for the experimental groups and likewise, where *C* and *C*₀ are the mean tumor volumes for the control group.

In Vitro Metabolic Stability in Liver Microsomes. Microsomal stability assay: 1 μ M of each compound was incubated with human (or mouse) liver microsome (0.5 mg protein/mL) in 50 mM phosphate buffer (pH 7.4) containing 1 mM NADPH (the reduced form of nicotinamide adenine dinucleotide phosphate) at 37 °C for 30 min. After the enzyme reaction was terminated with the addition of a 3-fold

volume of acetonitrile, the reaction mixture was centrifuged at 1500 rpm for 10 min. The resultant supernatant was used as a test sample to measure the stability in human (or mouse) liver microsome by quantitating the compound in the sample using LC/MS.

Determination of Pharmacokinetic Parameters in Monkeys. Fasted cynomolgus monkeys ($n = 2$ per treatment group) were given **13d** by oral (po) or intravenous (iv) route at a dose of 0.5 mg/kg. Compound **13d** was dissolved in a vehicle of 20% EtOH, 10% Cremophor EL, 15% PEG400, 15% HPCD (2-hydroxypropyl- β -cyclodextrin), and 0.02 mol/L HCl in water. Blood samples were collected with heparin as an anticoagulant at 0.08, 0.25, 1, 2, 4, 7, 24, and 48 h following iv dosing and at 0.50, 1, 2, 4, 7, 24, and 48 h following oral dosing. Samples were centrifuged and the plasma collected and stored at –80 °C until analysis. Samples were analyzed by LC-MS/MS technique. The pharmacokinetic parameters were calculated by noncompartmental analysis.

■ ASSOCIATED CONTENT

S Supporting Information. Experimental conditions for enzyme assays. IC₅₀ values of Table 1 in each assay. Amino acid sequences of the 14 kinases having AG at the E₀ region. Pharmacokinetic study of **13d** in mice. This material is available free of charge via the Internet at <http://pubs.acs.org>.

■ AUTHOR INFORMATION

Corresponding Author

*Phone: +81(467)47-6050. Fax: +81(467)47-2248. E-mail: kinoshitakzt@chugai-pharm.co.jp.

■ ACKNOWLEDGMENT

We thank Y. Tachibana, K. Sakata, and T. Fujii for biological assays, K. H. Ahn for chemical synthesis, S. Kuramoto and N. Shibahara for PK analysis, Y. Akada, M. Hiramoto and K. Yoshinari for physicochemical assays, and H. Suda, F. Matsuno and Y. Ishiguro for mass spectrometry measurements.

■ ABBREVIATIONS USED

ALCL, anaplastic large cell lymphomas; ALK, anaplastic lymphoma kinase; Boc, *t*-butoxycarbonyl; CL, clearance; CPME, cyclopropyl methyl ether; DDQ, 2,3-dichloro-5,6-dicyanobenzoquinone; DLBCL, diffuse large B-cell lymphoma; DME, 1,2-dimethoxyethane; DMF, *N,N*-dimethylformamide; DMSO, dimethylsulfoxide; EGFR, epidermal growth factor receptor; EML4, echinoderm microtubule-associated protein-like 4; IGF-1R, insulin-like growth factor-1 receptor; IMT, inflammatory myofibroblastic tumor; INSR, insulin receptor; KDR, kinase insert domain receptor; KRAS, v-K_i-ras2 Kirsten rat sarcoma viral oncogene homologue; LTK, leukocyte tyrosine kinase; NADPH, nicotinamide adenine dinucleotide phosphate; NMP, *N*-methyl pyrrolidone; NSCLC, non-small cell lung cancer; PDB, Protein Data Bank; RTK, receptor tyrosine kinase; SCC, squamous cell carcinoma; TBAF, tetrabutylammonium fluoride; TFA, trifluoroacetic acid; TGI, tumor growth inhibition; THF, tetrahydrofuran; TIPS, triisopropylsilyl

■ REFERENCES

(1) Morris, S. W.; Naeve, C.; Mathew, P.; James, P. L.; Kirstein, M. N.; Cui, X.; Witte, D. P. *ALK, The Chromosome 2 Gene Locus Altered by the t(2;5) in Non-Hodgkin's Lymphoma, Encodes a Novel Neural Receptor Tyrosine Kinase That Is Highly Related to Leukocyte Tyrosine Kinase (LTK)*. *Oncogene* **1997**, *14*, 2175–2188.

- (2) Pulford, K.; Lamant, L.; Morris, S. W.; Butler, L. H.; Wood, K. M.; Stroud, D.; Delsol, G.; Mason, D. Y. Detection of Anaplastic Lymphoma Kinase (ALK) and Nucleolar Protein Nucleophosmin (NPM)-ALK Proteins in Normal and Neoplastic Cells with the Monoclonal Antibody ALK1. *Blood* **1997**, *89*, 1394–1404.
- (3) Morris, S. W.; Kirstein, M. N.; Valentine, M. B.; Dittmer, K. G.; Shapiro, D. N.; Saltman, D. L.; Look, A. T. Fusion of a Kinase Gene, ALK, to a Nucleolar Protein Gene, NPM, in Non-Hodgkin's Lymphoma. *Science* **1994**, *263*, 1281–1284.
- (4) Li, R.; Morris, S. W. Development of Anaplastic Lymphoma Kinase (ALK) Small-Molecule Inhibitors for Cancer Therapy. *Med. Res. Rev.* **2008**, *28*, 372–412.
- (5) Webb, T. R.; Slavish, J.; George, R. E.; Look, A. T.; Xue, L.; Jiang, Q.; Cui, X.; Rentrop, W. B.; Morris, S. W. Anaplastic Lymphoma Kinase: Role in Cancer Pathogenesis and Small-Molecule Inhibitor Development for Therapy. *Expert Rev. Anticancer Ther.* **2009**, *9*, 331–356.
- (6) Griffin, C. A.; Hawkins, A. L.; Dvorak, C.; Henkle, C.; Ellingham, T.; Perlman, E. J. Recurrent Involvement of 2p23 in Inflammatory Myofibroblastic Tumors. *Cancer Res.* **1999**, *59*, 2776–2780.
- (7) Gascoyne, R. D.; Lamant, L.; Martin-Subero, J. I.; Lestou, V. S.; Harris, N. L.; Muller-Hermelink, H. K.; Seymour, J. F.; Campbell, L. J.; Horsman, D. E.; Auvigne, I.; Espinos, E.; Siebert, R.; Delsol, G. ALK-Positive Diffuse Large B-cell Lymphoma is Associated with *Clathrin-ALK* Rearrangements: Report of 6 Cases. *Blood* **2003**, *102*, 2568–2573.
- (8) Jazii, F. R.; Najafi, Z.; Malekzadeh, R.; Conrads, T. P.; Ziaee, A. A.; Abnet, C.; Yazdznbod, M.; Karkhane, A. A.; Salekdeh, G. H. Identification of Squamous Cell Carcinoma Associated Proteins by Proteomics and Loss of Beta Tropomyosin Expression in Esophageal Cancer. *World J. Gastroenterol.* **2006**, *12*, 7104–7112.
- (9) Soda, M.; Choi, Y. L.; Enomoto, M.; Takada, S.; Yamashita, Y.; Ishikawa, S.; Fujiwara, S.; Watanabe, H.; Kurashina, K.; Hatanaka, H.; Bando, M.; Ohno, S.; Ishikawa, Y.; Aburatani, H.; Niki, T.; Sohara, Y.; Sugiyama, Y.; Mano, H. Identification of the Transforming *EML4-ALK* Fusion Gene in Non-small-cell Lung Cancer. *Nature* **2007**, *448*, 561–566.
- (10) Mano, H. Non-solid Oncogenes in Solid Tumors: *EML4-ALK* Fusion Genes in Lung Cancer. *Cancer Sci.* **2008**, *99*, 2349–2355.
- (11) Koivunen, J. P.; Mermel, C.; Zejnullahu, K.; Murphy, C.; Lifshits, E.; Holmes, A. J.; Choi, H. G.; Kim, J.; Chiang, D.; Thomas, R.; Lee, J.; Richards, W. G.; Sugarbaker, D. J.; Ducko, C.; Lindeman, N.; Marcoux, J. P.; Engelman, J. A.; Gray, N. S.; Lee, C.; Meyerson, M.; Jänne, P. A. *EML4-ALK* Fusion Gene and Efficacy of an ALK Kinase Inhibitor in Lung Cancer. *Clin. Cancer Res.* **2008**, *14*, 4275–4283.
- (12) Inamura, K.; Takeuchi, K.; Togashi, Y.; Hatano, S.; Ninomiya, H.; Motoi, N.; Mun, M. Y.; Sakao, Y.; Okumura, S.; Nakagawa, K.; Soda, M.; Choi, Y. L.; Mano, H.; Ishikawa, Y. *EML4-ALK* Lung Cancers Are Characterized by Rare Other Mutations, A TTF-1 Cell Lineage, An Acinar Histology, and Young Onset. *Mod. Pathol.* **2009**, *22*, 508–515.
- (13) Osajima-Hakomori, Y.; Miyake, I.; Ohira, M.; Nakagawara, A.; Nakagawa, A.; Sakai, R. Biological Role of Anaplastic Lymphoma Kinase in Neuroblastoma. *Am. J. Pathol.* **2005**, *167*, 213–222.
- (14) Mossé, Y. P.; Laudenslager, M.; Longo, L.; Cole, K. A.; Wood, A.; Attiye, E. F.; Laquaglia, M. J.; Sennett, R.; Lynch, J. E.; Perri, P.; Laureys, G.; Speleman, F.; Kim, C.; Hou, C.; Hakonarson, H.; Torkamani, A.; Schork, N. J.; Brodeur, G. M.; Tonini, G. P.; Rappaport, E.; Devoto, M.; Maris, J. M. Identification of *ALK* as a Major Familial Neuroblastoma Predisposition Gene. *Nature* **2008**, *455*, 930–935.
- (15) Kumar, R.; Crouthamel, M.-C.; Rominger, D. H.; Gontarek, R. R.; Tummino, P. J.; Levin, R. A.; King, A. G. Myelosuppression and Kinase Selectivity of Multikinase Angiogenesis Inhibitors. *Br. J. Cancer* **2009**, *101*, 1717–1723.
- (16) Izzedine, H.; Rixe, O.; Billefont, B.; Baumelou, A.; Deray, G. Angiogenesis Inhibitor Therapies: Focus on Kidney Toxicity and Hypertension. *Am. J. Kidney Dis.* **2007**, *50*, 203–218.
- (17) Rodig, S. J.; Shapiro, G. I.; Crizotinib, A Small-Molecule Dual Inhibitor of the c-Met and ALK Receptor Tyrosine Kinases. *Curr. Opin. Invest. Drugs* **2010**, *11*, 1477–1490.
- (18) Kinoshita, K.; Ono, Y.; Emura, T.; Asoh, K.; Furuichi, N.; Ito, T.; Kawada, H.; Tanaka, S.; Morikami, K.; Tsukaguchi, T.; Sakamoto, H.; Tsukuda, T.; Oikawa, N. Discovery of Novel Tetracyclic Compounds as Anaplastic Lymphoma Kinase Inhibitors. *Bioorg. Med. Chem. Lett.* **2011**, *21*, 3788–3793.
- (19) Kinoshita, K.; Asoh, K.; Furuichi, N.; Ito, T.; Kawada, H.; Ishii, N.; Sakamoto, H.; Hong, W. S.; Park, M. J.; Ono, Y.; Kato, Y.; Morikami, K.; Emura, T.; Oikawa, N. Tetracyclic Compound. *PCT Int. Appl. WO2010/143664*, 2010.
- (20) Hart, H.; Corbin, J. L.; Wagner, C. R.; Wu, C.-Y. Alkylation of Phenol with a Homoallylic Halide. *J. Am. Chem. Soc.* **1963**, *85*, 3269–3273.
- (21) Liao, J. J. L. Molecular Recognition of Protein Kinase Binding Pockets for Design of Potent and Selective Kinase Inhibitors. *J. Med. Chem.* **2007**, *50*, 409–424.
- (22) This is the result of our kinase database search. The names and amino acid sequences of ATP binding pocket of the 14 kinases are described in Supporting Information.
- (23) Sakamoto, H.; Tsukaguchi, T.; Hiroshima, S.; Kodama, T.; Kobayashi, T.; Fukami, T. A.; Oikawa, N.; Tsukuda, T.; Ishii, N.; Aoki, Y. CH5424802, a Selective ALK Inhibitor Capable of Blocking the Resistant Gatekeeper Mutant. *Cancer Cell* **2011**, *19*, 679–690.
- (24) The complex model was prepared using the Molecular Operating Environment software package (MOE 2010.10; Chemical Computing Group Inc., Montreal, Quebec). The cocrystal structure of human ALK in complex with CH5424802 (PDB code 3AOX) was used to construct complex models of compound **13a**. Compound **13a** was derived by modifying the original ligand. The missing atoms of human ALK were constructed with reference to other human ALK crystal structures (PDB codes 3LCS and 2XP2). Solvent molecules within a distance of 5.0 Å around the original ligand were kept. All hydrogen atoms and modified parts of ligand were subjected to energy minimization using MMFF94x force field parameters in combination with GBSA solvent model. The final root-mean-square gradient was set to 0.001.
- (25) Fischer, P.; Nacheva, E.; Mason, D. Y.; Sherrington, P. D.; Hoyle, C.; Hayhoe, F. G.; Karpas, A. A Ki-1 (CD30)-positive Human Cell Line (Karpas 299) Established from a High-Grade Non-Hodgkin's Lymphoma, Showing a 2;5 Translocation and Rearrangement of the T-Cell Receptor Beta-Chain Gene. *Blood* **1988**, *72*, 234–240.